# Inelastic scattering $E4$ transition probabilities in the $0d$, $1s$ shell

B. A. Brown
*Nuclear Physics Laboratory, Oxford University, Oxford OX1 3RH, England*

W. Chung
*Cyclotron Laboratory, Michigan State University, East Lansing, Michigan 48824*

B. H. Wildenthal
*Nuclear Physics Laboratory, Oxford University, Oxford OX1 3RH, England*
*and Cyclotron Laboratory, Michigan State University,* East Lansing, Michigan 48824*

(Received 25 January 1980)

Theoretical $E4$ transition matrix elements calculated in the full $d_{5/2}$-$s_{1/2}$-$d_{3/2}$ shell-model space are presented for excitations of some ground states of stable nuclei for $18 \leq A \leq 38$. These matrix elements have been used to calculate inelastic transition probabilities for electromagnetic and hadronic probes. Available data on the relative magnitudes and energy distributions of $E4$ excitation strengths are found to be well reproduced theoretically thereby. Based on several experimentally measured transition strengths, the empirical isoscalar $E4$ effective charge is found to be $e_p + e_n = (2.0 \pm 0.2)e$. This is similar in magnitude to the analogous isoscalar $E2$ effective charge, but is much larger than existing theoretical estimates.

[NUCLEAR STRUCTURE $^{18}$O, $^{19}$F, $^{20}$Ne, $^{22}$Ne, $^{24}$Mg, $^{25}$Mg, $^{26}$Mg, $^{28}$Si, $^{30}$Si, $^{32}$S, $^{34}$S, $^{36}$Ar, $^{38}$Ar; calculations for the strengths of $E4$ inelastic scattering transitions and their proton and neutron components; complete $0d_{5/2}$-$1s_{5/2}$-$0d_{3/2}$ shell-model wave functions; Chung-Wildenthal Hamiltonians.]

## I. INTRODUCTION

In this paper we present calculations for the strengths of $\Delta J^\pi = 4^+(E4)$ excitations of ground states in the region $18 \leq A \leq 38$. The one-body transition density matrix elements for these excitations were calculated from the $d_{5/2}$-$s_{1/2}$-$d_{3/2}$ shell-model wave functions of Chung and Wildenthal.[1,2] These transition densities were then used to calculate matrix elements for electromagnetic excitation of these transitions and for the relative strengths of these same transitions as they are excited by various hadronic probes. The present calculations systematically employ harmonic-oscillator single-particle wave functions. The effects of using different (e.g., Hartree-Fock) radial dependences for the single-particle states were examined and found to be significant, but no alternative clearly preferable to harmonic-oscillator dependence was determined.

Our present study focuses on three aspects of $E4$ phenomena. The first issue we address presumes reasonably good theoretical-experimental agreement between *relative* values of several large measured transition strengths. In such a context it is meaningful to speak of the "effective charges" appropriate to the model space which serve to produce agreement between calculation and experiment in the absolute as well as relative sense. By comparing values from the extant body of measured $E4$ rates to our calculated values we are able to extract a value of the isoscalar $E4$ effective charge for the $sd$-shell space of $e_p + e_n = (2.0 \pm 0.2)e$.

We then proceed to deal with the general questions of what type of $E4$ phenomena are predicted by the Chung-Wildenthal wave functions and how well these accord with experimental facts. There are several aspects to be considered, such as the dependence of the aggregate $E4$ strength on the $A$ value, the distribution of strength within a given nucleus as a function of excitation energy, and the $A$ dependence of this distribution.

Lastly, we consider the individual neutron and proton components of the transitions in the $T \neq 0$ nuclei. From the values of these components the relative strengths by which a given state is excited by various hadronic probes, as well as electronmagnetically, can be predicted. We consider in particular, alphas, protons, and pions.

In Sec. II the calculation of the shell-model transition-density matrix elements is described as well as their combination with the single-particle matrix elements (which incorporate the radial wave function dependence) to obtain the theoretical $B(E4)$ values. In Sec. III these values are compared with the strong experimental $B(E4)$ values to obtain $E4$ effective charges. In addition, the

 

distributions of calculated $E4$ strengths for all stable even-even nuclei are presented in comparison with available experimental data, together with some selected results for odd-even nuclei. In Sec. IV a method for calculating the hadronic excitation strengths is presented. The conclusions of the present study constitute Sec. V.

## II. SHELL-MODEL CALCULATIONS OF THE TRANSITION DENSITIES

The reduced matrix element for a one-body operator between initial and final $sd$-shell wave functions for $N$ valence particles is expressed as a linear combination of reduced matrix elements between single-particle states $\rho_j$ and the one-body transition densities $D^{N,JT,J'T'}_{\Delta T,\Delta T}$ by the relation

$$\left\langle \psi^{NJT}\middle|\middle|\middle| \sum_{i=1}^{N} O(\Delta J,\Delta T)\middle|\middle|\middle| \psi^{NJ'T'}\right\rangle = \sum_{jj'} D^{N,JT,J'T'}_{\Delta T,\Delta T}(j,j')\langle \rho_j|||O(\Delta J,\Delta T)|||\rho_{j'}\rangle , \tag{1}$$

where

$$D^{N,JT,J'T'}_{\Delta T,\Delta T}(j,j')=\frac{\langle \psi^{NJT}|||(a_j^{\dagger}\times \tilde{a}_{j'})_{\Delta J\Delta T}|||\psi^{NJ'T'}\rangle}{[(2\Delta J+1)(2\Delta T+1)]^{1/2}} . \tag{2}$$

The operator $O(\Delta J,\Delta T)$ has associated with it a unit operator in isospin space when $\Delta T=0$ and the operator $\tau$ in isospin space when $\Delta T=1$; our isospin convention is such that

$$O(\Delta J)_{p/n}=\tfrac{1}{2}[1(+/-)\tau_3]O(\Delta J) . \tag{3}$$

The proton and neutron matrix elements for these operators between the $sd$-shell wave functions are given by

$$A_{p/n}(T_z)=\frac{(-1)^{T_f-T_z}}{2}\begin{pmatrix} T_f & 0 & T_i \\ -T_z & 0 & T_z\end{pmatrix}\left\langle \psi^{J_fT_f}\middle|\middle|\middle| \sum_{i=1}^{N} O(\Delta J,\Delta T=0)_i\middle|\middle|\middle| \psi^{J_iT_i}\right\rangle$$
$$(+/-)\frac{(-1)^{T_f-T_z}}{2}\begin{pmatrix} T_f & 1 & T_i \\ -T_z & 0 & T_z\end{pmatrix}\left\langle \psi^{J_fT_f}\middle|\middle|\middle| \sum_{i=1}^{N} O(\Delta J,\Delta T=1)_i\middle|\middle|\middle| \psi^{J_iT_i}\right\rangle . \tag{4}$$

It is well known in the case of $E2$ transitions that core-polarization corrections are important and we anticipate that they will also be important for $E4$ transitions. Thus we introduce proton and neutron effective charges $e_p$ and $e_n$ which relate the total proton matrix element $M_p$ to the proton and neutron matrix elements in the model space $A_p$ and $A_n$:

$$M_p=A_pe_p+A_ne_n=A_p(1+\delta e_p)+A_n\delta e_n . \tag{5}$$

In terms of $M_p$ the $B(E4)$ value is given by

$$B(E4,J_i\to J_f)=(2J_i+1)^{-1}M_p^{\,2} . \tag{6}$$

The quantity $\delta e_p$ represents the effect of virtual excitation of core protons by the valence protons and the quantity $\delta e_n$ represents the effect of the virtual excitation of core protons by the valence neutrons. If we denote $\delta e_p$ by $\delta_{pp}$ and $\delta e_n$ by $\delta_{pn}$, then the generalizations of Eq. (5) for both the proton and neutron matrix elements take the form

$$\begin{aligned} M_p&=A_p(1+\delta_{pp})+A_n\delta_{pn} ,\\ M_n&=A_n(1+\delta_{nn})+A_p\delta_{np} .\end{aligned} \tag{7}$$

(The neutron matrix elements will be needed to calculate strengths for hadronic excitations.) For nuclei with approximately equal numbers of neutrons and protons $\delta_{np}=\delta_{pn}$ and, since the nuclear interaction is charge symmetric, $\delta_{nn}=\delta_{pp}$. Thus we can express the neutron matrix element in terms of the proton and neutron effective charges,

$$M_n=A_ne_p+A_pe_n . \tag{8}$$

The values of the one-body transition densities $D$ for some of the transitions discussed in the following sections are given in Table I. These quantities constitute the total information content of the shell-model wave functions insofar as these $E4$ excitations are concerned. The matrix elements

$$\left\langle \psi^{NJT}\middle|\middle|\middle| \sum_{i=1}^{N} O(\Delta J,\Delta T)_i\middle|\middle|\middle| \psi^{NJ'T'}\right\rangle$$

or the equivalent $A_{p/n}$ can be calculated from these entries once a set of single-particle matrix elements are specified.

The triply reduced single-particle matrix elements are

$$\langle \rho_j|||O(\Delta J,\Delta T=0)|||\rho_{j'}\rangle=(2)^{1/2}\langle \rho_j||O(\Delta J)||\rho_{j'}\rangle$$

and

$$\langle \rho_j|||O(\Delta J,\Delta T=1)|||\rho_{j'}\rangle=(6)^{1/2}\langle \rho_j||O(\Delta J)||\rho_{j'}\rangle . \tag{9}$$

The electric multipole operator is given by

$$O(\Delta J)_i=r_i^{\Delta J}Y_m^{(\Delta J)}(\hat{r}_i) . \tag{10}$$

TABLE I. Calculated values of the one-body transition densities for some selected $E4$ transitions.

| A | $T_i \to T_f$ | $J_i \to J_f$ | $j$-$j'$ $\Delta T=0$ $\frac{5}{2}$-$\frac{5}{2}$ | $\frac{5}{2}$-$\frac{3}{2}$ | $\frac{3}{2}$-$\frac{5}{2}$ | $\Delta T=1$ $\frac{5}{2}$-$\frac{5}{2}$ | $\frac{5}{2}$-$\frac{3}{2}$ | $\frac{3}{2}$-$\frac{5}{2}$ |
|---|---|---|---|---|---|---|---|---|
| 18 | $1\to1$ | $0^+\to4^+(1)$ | −0.8266 | −0.0726 | 0.1817 | −0.6749 | −0.0593 | 0.1483 |
| 19 | $\frac{1}{2}\to\frac{1}{2}$ | $\frac{1}{2}^+\to\frac{9}{2}^+(1)$ | 0.4483 | 0.3411 | −0.1715 | 0.2395 | −0.0377 | −0.1721 |
| 20 | $0\to0$ | $0^+\to4^+(1)$ | 0.4033 | 0.2714 | −0.3061 | | | |
| | | $0^+\to4^+(2)$ | 0.0141 | −0.1054 | 0.0695 | | | |
| 22 | $1\to1$ | $0^+\to4^+(1)$ | −0.0210 | −0.2009 | 0.3206 | 0.6233 | 0.0303 | −0.0638 |
| | | $0^+\to4^+(2)$ | 0.8423 | 0.0269 | −0.2217 | 0.3384 | −0.0610 | −0.0218 |
| 24 | $0\to0$ | $0^+\to4^+(1)$ | −0.3057 | −0.0076 | −0.0426 | | | |
| | | $0^+\to4^+(2)$ | 0.2402 | 0.3082 | −0.4845 | | | |
| | | $0^+\to4^+(3)$ | 0.3469 | −0.0976 | 0.0327 | | | |
| 25 | $\frac{1}{2}\to\frac{1}{2}$ | $\frac{5}{2}^+\to\frac{9}{2}^+(1)$ | 0.4962 | −0.2212 | 0.0778 | −0.1159 | −0.0182 | 0.0257 |
| | | $\frac{5}{2}^+\to\frac{9}{2}^+(2)$ | 0.2396 | 0.4615 | −0.2587 | −0.0123 | 0.0056 | 0.0323 |
| | | $\frac{5}{2}^+\to\frac{13}{2}^+(3)$ | −0.2156 | −0.2610 | 0.5347 | 0.1647 | 0.0585 | −0.0318 |
| 26 | $1\to1$ | $0^+\to4^+(1)$ | 0.7231 | 0.1225 | −0.3194 | −0.5609 | 0.0920 | −0.1292 |
| | | $0^+\to4^+(2)$ | −0.0417 | −0.3206 | 0.7093 | 0.0043 | −0.0235 | 0.1286 |
| | | $0^+\to4^+(3)$ | 0.1833 | 0.1277 | −0.2988 | 0.3690 | −0.0097 | −0.1744 |
| 28 | $0\to0$ | $0^+\to4^+(1)$ | −0.0065 | −0.4561 | 0.2478 | | | |
| | | $0^+\to4^+(2)$ | 0.2267 | 0.4496 | −0.1517 | | | |
| | | $0^+\to4^+(3)$ | −0.2008 | 0.1694 | −0.1190 | | | |
| 30 | $1\to1$ | $0^+\to4^+(1)$ | 0.2305 | 0.6219 | −0.3076 | −0.0978 | 0.3469 | −0.1662 |
| | | $0^+\to4^+(2)$ | −0.1606 | −0.8941 | 0.3455 | −0.0534 | 0.2664 | −0.0551 |
| | | $0^+\to4^+(3)$ | −0.0122 | −0.0787 | −0.0178 | 0.3036 | 0.3685 | −0.0363 |
| 32 | $0\to0$ | $0^+\to4^+(1)$ | −0.0911 | −0.5652 | 0.3328 | | | |
| | | $0^+\to4^+(2)$ | 0.0917 | 0.3303 | −0.1418 | | | |
| | $0\to1$ | $0^+\to4^+(2)$ | | | | 0.0288 | 0.4918 | −0.0858 |
| 34 | $1\to1$ | $0^+\to4^+(1)$ | 0.1361 | 0.8449 | −0.4448 | 0.0049 | −0.0445 | −0.0372 |
| | | $0^+\to4^+(2)$ | −0.1047 | 0.1241 | −0.0464 | −0.0690 | −0.3905 | 0.1371 |
| 36 | $0\to0$ | $0^+\to4^+(1)$ | −0.1252 | −0.4596 | 0.3211 | | | |
| | $0\to1$ | $0^+\to4^+(3)$ | | | | −0.0089 | −0.4011 | 0.1070 |
| 38 | $1\to1$ | $0^+\to4^+(1)$ | −0.0345 | −0.8156 | 0.1947 | 0.0281 | 0.6659 | −0.1589 |

For $\Delta J=4$ there are only two possible independent single-particle matrix elements in the $sd$-shell space and these are given by

$$\langle d_{5/2}||r^4Y^{(4)}||d_{5/2}\rangle=\left(\frac{9}{7\pi}\right)^{1/2}\langle d_{5/2}|r^4|d_{5/2}\rangle\,,$$
$$\langle d_{5/2}||r^4Y^{(4)}||d_{3/2}\rangle=\left(\frac{18}{7\pi}\right)^{1/2}\langle d_{5/2}|r^4|d_{3/2}\rangle\,. \tag{11}$$

Since the $E4$ matrix elements are weighted by $r^4$, the relation between experiment and theory is very sensitive to the specification of the radial integrals in Eqs. (11). We have chosen to evaluate these integrals independently for each nucleus we consider by choosing harmonic-oscillator wave functions parametrized to reproduce the individual measured values of the rms charge radii. The rms charge radii $r_{ch}$ for essentially all stable $sd$-shell nuclei are now known to high accuracy, a rather recent development. These values are

TABLE II. Rms charge radii and the extracted harmonic oscillator parameter $b$.

| | $r_{ch}$ (fm) | $b$ (fm) | $\hbar\omega$ (MeV) |
|---|---|---|---|
| $^{18}$O | 2.794(3)[a] | 1.820 | 12.50 |
| $^{19}$F | 2.898(10)[b] | 1.833 | 12.34 |
| $^{20}$Ne | 3.020(20)[c] | 1.869 | 11.87 |
| $^{22}$Ne | 2.949(20)[d] | 1.821 | 12.50 |
| $^{24}$Mg | 3.035(18)[e] | 1.813 | 12.61 |
| $^{25}$Mg | 3.003(11)[f] | 1.793 | 12.90 |
| $^{26}$Mg | 3.017(32)[g] | 1.802 | 12.77 |
| $^{28}$Si | 3.127(3)[b,h] | 1.827 | 12.42 |
| $^{30}$Si | 3.139(3)[i] | 1.834 | 12.33 |
| $^{32}$S | 3.264(2)[b] | 1.881 | 11.72 |
| $^{34}$S | | 1.881 | 11.72 |
| $^{36}$Ar | 3.399(5)[i] | 1.938 | 11.04 |
| $^{38}$Ar | 3.414(10)[j] | 1.947 | 10.94 |

[a] Reference 26.
[b] Reference 27.
[c] Reference 28, Table I.
[d] Reference 10; $r_{ch}(^{22}\text{Ne}) - r_{ch}(^{20}\text{Ne}) = -0.071$ fm.
[e] Reference 29.
[f] Reference 30.
[g] Reference 28, Table II.
[h] For natural Si, $r_{ch} = 3.129$ (3).
[i] Reference 31, Table IV.
[j] Reference 31, Table III.

listed in Table II.

For the harmonic-oscillator potential $V(r) = \frac{1}{2}m\omega^2 r^2$, the point proton rms radius for nuclei in the $sd$ shell is given by

$$r_p^2 = \left[\frac{18 + (Z-8)\frac{7}{2}}{Z}\right] b^2 - \frac{3b^2}{2A},$$

where

$$b^2 = \hbar/m\omega. \tag{12}$$

The last term is the correction for center-of-mass motion.[3,4] The charge radius is obtained by folding $r_p$ with the rms charge radii for the protons and neutrons and adding relativistic corrections. Ignoring the relativistic spin-orbit correction, which is important only for nuclei with a large neutron or proton excess of spin unsaturated nucleons, the rms charge radii are given by[3]

$$r_{ch}^2 = r_p^2 + r_{proton}^2 + \frac{N}{Z} r_{neutron}^2 + \frac{3}{4}\left(\frac{\hbar}{mc}\right)^2, \tag{13}$$

where $r_{proton}^2 = (0.86)^2$ and $r_{neutron}^2 = -(0.35)^2$. The values of $b$ and $\hbar\omega$ extracted from the experimental charge radii are given in Table II. In terms of $b$, the radial matrix elements of Eqs. (11) are expressed as

$$\langle d_{5/2}|r^4|d_{5/2}\rangle = \langle d_{5/2}|r^4|d_{3/2}\rangle = 15.75b^4. \tag{14}$$

The procedure we have adopted obviously takes into account all of the new precisely known variations in the sizes of $sd$-shell ground states. The conventional prescriptions for either harmonic-oscillator or Saxon-Woods potentials, which assume some smoothly varying mass dependence, e.g., $\hbar\omega = 41A^{-1/3}$, fail to account for these variations, sometimes by significant amounts. In our opinion it is appropriate to remove this source of noise in the comparison of theoretical to experimental elements by abandoning size formulas altogether and using instead the individual measured radii.

We utilize harmonic-oscillator radial dependence rather than Saxon-Woods or Hartree-Fock prescriptions because these latter, supposedly more "realistic," presciptions do not in fact offer improvements over the harmonic oscillator sufficient to justify the additional complexity and ambiguity their use introduces into the problems at hand. The problem inherent in specifying single-particle wave functions for open-shell nuclei such as concern us here is that the experimental separation energies are inconsistent with the energies of the shell-model single-particle potential, e.g., for $^{28}$Si the $1s_{1/2}$ separation energy is greater than that for $0d_{5/2}$, and $0d_{3/2}$ is greater than $1s_{1/2}$, in inverse order to the shell-model sequence. In the full shell-model calculation this effect comes out of the two-body part of the Hamiltonian, but simple single-particle models are helpless to deal with it. Moreover, by going from the infinite harmonic-oscillator well to finite wells, one runs the risk of obtaining more realistic surface behavior in some wave functions at the cost of introducing more serious errors in others.

In our judgement it is advisable to retain the advantages of harmonic-oscillator dependence, where possible, until rigorous treatments of the single-particle problem, treatments which will presumbably follow along the paths explored in the treatment of single-nucleon transfer reactions,[5] become available. At the same time, it is also advisable to ascertain the degree to which conclusions based on the harmonic oscillator are subject to change when alternate models are used. To this end we have explored the consequence of using the radial-matrix elements of $r^4$ which are obtained from the Hartree-Fock calculations of Brown and Massen.[6] Some results from this study are presented in the Appendix.

## III. RESULTS AND COMPARISON WITH EXPERIMENT

We first consider the strongest experimentally measured $E4$ transitions together with the matrix elements $A_p$ and $A_n$ in order to determine the empirical effective charges from the relationship

$$B(E4) = (2J_i + 1)^{-1} M_p^2$$
$$= (2J_i + 1)^{-1} (A_p e_p + A_n e_n)^2.$$

This comparison is made in Table III in which the matrix elements $M_p$ have been rewritten in the form

$$M_p = \tfrac{1}{2}(A_p + A_n)(e_p + e_n) + \tfrac{1}{2}(A_p - A_n)(e_p - e_n) \quad (15)$$

in order to show that the isovector quantity $A_p - A_n$ is usually small relative to the isoscalar quantity $A_p + A_n$. (An exception to this occurs in $^{22}$Ne.) For this reason $e_p - e_n$ cannot be reliably determined from the existing experimental data and we have set it equal to the bare value $e_p - e_n = e$.

The values of $e_p + e_n$ which serve to equate the shell-model predictions to the measured value for each experimentally observed transition are listed as the last column in Table III. All cluster around a value of $e_p + e_n = 2.0e$. This empirical value is much larger than the theoretical value of $e_p + e_n = 1.15e$ calculated by Horikawa *et al.*[7] Part of this discrepancy may be due to the fact that Horikawa *et al.* assumed unperturbed energies ($\Delta E \simeq 2\hbar\omega$, $4\hbar\omega, \ldots$) for the one-particle–one-hole states and if there were a collective "giant" $4^+$, $T = 0$ state it could occur lower in energy, which would thus enhance its admixture into the model-space wave functions and make the isoscalar effective charge larger.

Analyses of the experimentally measured $B(E4)$ for the $\frac{19}{2}^- \rightarrow \frac{11}{2}^-$ transition in $^{53}$Fe have suggested that the $E4$ effective charge is small and the $E6$ effective charge is even negative.[8] The present results suggest that these "anomalies" in $^{53}$Fe may originate within the valence ($fp$) shell configurations via effects which have not been accurately calculated in previous shell-model calculations because of the large dimensions involved, rather than being a consequence of systematic, state-independent quenching of the effective charge.

We present in Tables IV–VII calculated energies and values of $A_p$, $A_n$, $M_p$, $M_n$, and $B(E4)$ for $\Delta J^\pi = 4^+$ excitations, along with what experimental information exists. Rather complete sets of predictions are given for $\Delta T = 0$ and $\Delta T = 1$ excitations in $N = Z$ nuclei (Tables IV and V, respectively) and for the $\Delta T = 0 + 1$ excitations of the $T = 1$ states in $T_Z = -1$ nuclei (Table VI). For stable even-odd nuclei we present (in Table VII) results only for $^{19}$F and $^{25}$Mg, for which some experimental data exist. The values of $M_p$, $M_n$, and $B(E4)$ are based upon the values of the added effective charges $\delta_{pp} = \delta_{nn} = \delta_{np} = \delta_{pn} = 0.5$ as motivated by the results of Table III.

In comparing theoretical and experimental values of $B(E4)$ it is important to note that there are several theoretical sources of uncertainty in the values quoted for the experimental $B(E4)$. The $B(E4)$ values are obtained from inelastic electron scattering data by an extrapolation of the form factors measured at finite values of the momentum transfer $q$ to the value for $q = \omega$ by using a model for the shape of the form factor. All results which we quote have been obtained with the Tassie model,[9] which is probably quite adequate for the strong $E4$ transitions but potentially questionable for the weak $E4$ transitions, where unusual shapes in the transition density may result from cancellation between single-particle form factors. In

TABLE III. Isoscalar effective charges for the stronger experimentally measured $E4$ transitions.

| | $J_i \rightarrow J_f$ | $[B(E4)]^{1/2}(e^2\text{fm}^4)$ Theory | Experiment[a] | $\frac{e_p + e_n}{e}$[b] |
|---|---|---|---|---|
| $^{19}$F | $\frac{1}{2}^+ \rightarrow \frac{9}{2}^+$ (1) | $46.8(e_p + e_n) - 17.2(e_p - e_n)$ | 69 ± 8 | 1.8 ± 0.2 |
| $^{20}$Ne | $0^+ \rightarrow 4^+$(1) | $106(e_p + e_n)$ | 195 ± 20 | 1.8 ± 0.2 |
| $^{22}$Ne | $0^+ \rightarrow 4^+$(1) | $34.4(e_p + e_n) + 42.0(e_p - e_n)$ | 130 ± 15 | 2.6 ± 0.4 |
| $^{24}$Mg | $0^+ \rightarrow 4^+$(2) | $105(e_p + e_n)$ | 207 ± 15 | 2.0 ± 0.2 |
| $^{26}$Mg | $0^+ \rightarrow 4^+$(2) | $65.0(e_p + e_n) - 11.2(e_p - e_n)$ | 161 ± 22 | 2.7 ± 0.3 |
| $^{28}$Si | $0^+ \rightarrow 4^+$(1) | $79.6(e_p + e_n)$ | 134 ± 7 | 1.7 ± 0.1 |

[a] For experimental references see Tables IV, VI, and VII.
[b] $(e_p - e_n) = e$ assumed.

TABLE IV. $\Delta T = 0$ $E4$ transitions in $N-Z$ nuclei.

| | $J_i \to J_f$ | $E_f$ (MeV) th | $E_f$ (MeV) exp[c] | $A_p$[a] (fm$^4$) | $M_p$[b] (fm$^4$) | $B(E4)$ ($e^2$fm$^8 \times 10^3$) th | $B(E4)$ ($e^2$fm$^8 \times 10^3$) exp | Method of exp. analysis |
|---|---|---|---|---|---|---|---|---|
| $^{20}$Ne | $0^+ \to 4^+(1)$ | 4.13 | 4.25[d] | 106.1 | 212 | 45 | $38 \pm 8$[e] | DUELS[h] |
| | $4^+(2)$ | 9.86 | 9.03[d] | −20.2 | −40 | 1.6 | | |
| | $4^+(3)$ | 10.97 | | −3.8 | −8 | 0.06 | | |
| | $4^+(4)$ | 11.70 | | −1.1 | −2 | 0.004 | | |
| | $4^+(5)$ | 14.29 | | −1.4 | −3 | 0.009 | | |
| | $4^+(6)$ | 14.63 | | 13.3 | 27 | 0.7 | | |
| $^{24}$Mg | $0^+ \to 4^+(1)$ | 4.42 | 4.12 | −19.7 | 39 | 1.6 | $2.0 \pm 0.3$[f] | DUELS[h] |
| | $4^+(2)$ | 5.89 | 6.01 | 104.9 | 210 | 44 | $43 \pm 6$[f] | DUELS[h] |
| | $4^+(3)$ | 8.79 | | 12.5 | 25 | 0.6 | | |
| | $4^+(4)$ | 9.62 | | −0.8 | 1.7 | 0.003 | | |
| | $4^+(5)$ | 11.15 | | 12.8 | 26 | 0.7 | | |
| | $4^+(6)$ | 12.18 | | −9.1 | −18 | 0.3 | | |
| | $4^+(7)$ | 12.25 | | −14.1 | −28 | 0.8 | | |
| | $4^+(8)$ | 12.63 | | −6.8 | −14 | 0.2 | | |
| $^{28}$Si | $0^+ \to 4^+(1)$ | 4.88 | 4.62 | −79.6 | −159 | 25 | $27 \pm 5$[g] | g |
| | $4^+(2)$ | 7.49 | 6.89 | 85.5 | 171 | 29 | | |
| | $4^+(3)$ | 9.70 | | 16.4 | 33 | 1.1 | | |
| | $4^+(4)$ | 10.15 | | 16.3 | 33 | 1.1 | | |
| | $4^+(5)$ | 10.50 | | −13.0 | −26 | 0.7 | | |
| | $4^+(6)$ | 11.06 | | 1.3 | 3 | 0.009 | | |
| | $4^+(7)$ | 11.29 | | −3.8 | −8 | 0.06 | | |
| | $4^+(8)$ | 11.93 | | 7.8 | 16 | 0.3 | | |
| $^{32}$S | $0^+ \to 4^+(1)$ | 4.82 | 4.46 | −121.4 | −243 | 59 | | |
| | $4^+(2)$ | 6.65 | 6.41 | 67.7 | 135 | 18 | | |
| | $4^+(3)$ | 7.55 | | 20.0 | 40 | 1.6 | | |
| | $4^+(4)$ | 7.94 | | −8.7 | −17 | 0.3 | | |
| | $4^+(5)$ | 9.00 | | 17.2 | 34 | 1.2 | | |
| | $4^+(6)$ | 9.36 | | −14.8 | −30 | 0.9 | | |
| | $4^+(7)$ | 9.98 | | 19.6 | 39 | 1.5 | | |
| | $4^+(8)$ | 10.40 | | 7.8 | 16 | 0.3 | | |
| $^{36}$Ar | $0^+ \to 4^+(1)$ | 4.74 | 4.41 | −123.5 | −248 | 62 | | |
| | $4^+(2)$ | 6.81 | | 3.3 | 6.5 | 0.04 | | |
| | $4^+(3)$ | 9.07 | | −30.5 | −61 | 3.7 | | |
| | $4^+(4)$ | 9.98 | | 18.6 | 37 | 14 | | |
| | $4^+(5)$ | 11.75 | | 16.6 | 33 | 1.1 | | |
| | $4^+(6)$ | 12.64 | | 22.7 | 45 | 2.0 | | |

[a] $A_n = A_p$.
[b] $M_n = M_p$.
[c] From Ref. 21 except where noted.
[d] Reference 32.
[e] Reference 10.
[f] Reference 11.
[g] The results given in Ref. 17 for the PWBA $B(E4)$ values in $^{24}$Mg and $^{28}$Si are $28.7 \times 10^3$ and $(17.8 \pm 2.0) \times 10^3$ $e^2$fm$^8$, respectively, whereas a DWBA value of $(43 \pm 6) \times 10^3$ $e^2$fm$^8$ is given in Ref. 11 for $^{24}$Mg. For $^{28}$Si we have used $B(E4) = [(43 \pm 6)/28.7] \times (17.8 \pm 2.0) \times 10^3$ $e^2$fm$^8$.
[h] Reference 16.

addition, the $E4$ transition strengths have been extracted from simple one-step, plane-wave Born approximation (PWBA) calculations. The results we quote from Refs. 10–15 have been corrected for distorted-wave effects with the computer code DUELS.[16] For a few cases, only the PWBA analysis is available (Refs. 17–19). $B(E2)$ values extracted from a distorted-wave Born approximation (DWBA) analysis are typically about 30% larger than those extracted from a PWBA analysis[17] and the difference is probably larger for $B(E4)$ values (see Sec. 5.5 in Ref. 15). Two-step excitations such as $0 \to 2 \to 4$ have not been considered and this must be important on some level for the transi-

TABLE V. $\Delta T = E4$ transitions in $N = Z$ nuclei.[a]

| | $J_i \to J_f$ | $E_f$ (MeV) th | $E_f$ (MeV) exp | $A_p$[b] (fm$^4$) | $M_p$[c] (fm$^4$) | $B(E4)$ ($e^2$fm$^8 \times 10^3$) th |
|---|---|---|---|---|---|---|
| $^{20}$Ne | $0^+ \to 4^+(1)\, T=1$ | 10.86 | 11.07[d] | 27.7 | 27.7 | 0.77 |
| | $4^+(2)\, T=1$ | 13.88 | | 8.4 | 8.4 | 0.07 |
| | $4^+(3)\, T=1$ | 15.74 | | −3.9 | −3.9 | 0.015 |
| | $4^+(4)\, T=1$ | 16.22 | | −9.7 | −9.7 | 0.09 |
| $^{24}$Mg | $0^+ \to 4^+(1)\, T=1$ | 9.74 | 9.51[e] | 16.4 | 16.4 | 0.27 |
| | $4^+(2)\, T=1$ | 12.28 | | 26.5 | 26.5 | 0.70 |
| | $4^+(3)\, T=1$ | 12.89 | | 25.1 | 25.1 | 0.63 |
| | $4^+(4)\, T=1$ | 13.36 | | −1.1 | −1.1 | 0.001 |
| $^{32}$S | $0^+ \to 4^+(1)\, T=1$ | 10.08 | 10.15[f] | −20.6 | −20.6 | 0.42 |
| | $4^+(2)\, T=1$ | 10.78 | | −75.5 | −75.5 | 5.7 |
| | $4^+(3)\, T=1$ | 11.85 | | 15.7 | 15.7 | 0.25 |
| | $4^+(4)\, T=1$ | 12.41 | | 26.3 | 26.3 | 0.69 |
| $^{36}$Ar | $0^+ \to 4^+(1)\, T=1$ | 10.32 | | −7.5 | −7.5 | 0.06 |
| | $4^+(2)\, T=1$ | 12.50 | | 31.0 | 31.0 | 0.96 |
| | $4^+(3)\, T=1$ | 12.76 | | 73.1 | 73.1 | 5.3 |
| | $4^+(4)\, T=1$ | 14.67 | | 13.3 | 13.3 | 0.18 |

[a] The theoretical results for $^{28}$Si have not been calculated.
[b] $A_n = -A_p$.
[c] $M_n = -M_p$.
[d] Reference 32.
[e] Based on the energy of the $1^+ T = 1$ state in $^{32}$S and the $4^+ T = 1$ state in $^{32}P$ (Ref. 21).
[f] Reference 21.

TABLE VI. $E4$ transitions for $T_z = -1$ nuclei ($T = 1 \to T = 1$).

| | $J_i \to J_f$ | $E_f$ (MeV) th | $E_f$ (MeV) exp[a] | $A_p$ (fm$^4$) | $A_n$ (fm$^4$) | $M_p$ (fm$^4$) | $M_n$ (fm$^4$) | $B(E4)$ ($e^2$fm$^8 \times 10^3$) th | $B(E4)$ ($e^2$fm$^8 \times 10^3$) exp | Method of exp analysis |
|---|---|---|---|---|---|---|---|---|---|---|
| $^{18}$O | $0^+ \to 4^+(1)$ | 3.52 | 3.56[b] | 0 | −107.1 | −54 | −161 | 2.9 | 1.04 ± 0.20[c] | DUELS[f] |
| | $4^+(2)$ | 8.21 | | 0 | −81.5 | −41 | −122 | 1.7 | | |
| $^{22}$Ne | $0^+ \to 4^+(1)$ | 3.42 | 3.36 | −76.3 | 7.6 | −111 | −27 | 12.3 | 17 ± 4[d] | DUELS[f] |
| | $4^+(2)$ | 5.40 | 5.52 | 38.4 | 69.7 | 92 | 124 | 8.5 | | |
| | $4^+(3)$ | 6.22 | 6.34 | −50.9 | −51.6 | −102 | −103 | 10.4 | | |
| | $4^+(4)$ | 7.21 | (7.34) | −13.9 | 62.9 | 11 | 87 | 0.3 | | |
| $^{26}$Mg | $0^+ \to 4^+(1)$ | 4.59 | 4.32 | 71.6 | 45.3 | 130 | 104 | 16.9 | | |
| | $4^+(2)$ | 5.41 | 4.90 | −53.8 | −76.2 | −119 | −141 | 14.1 | 26 ± 7[e] | DUELS[f] |
| | $4^+(3)$ | 5.87 | 5.47 | 2.1 | 66.1 | 36 | 100 | 1.3 | 3.4[e] | DUELS[f] |
| | $4^+(4)$ | 6.13 | 5.72 | −60.0 | −8.2 | −94 | −42 | 8.8 | 13 ± 5[e] | DUELS[f] |
| $^{30}$Si | $0^+ \to 4^+(1)$ | 5.40 | 5.28 | 36.1 | 107.6 | 108 | 180 | 11.7 | | |
| | $4^+(2)$ | 6.02 | 5.95 | 111.9 | 66.2 | 201 | 155 | 40 | | |
| | $4^+(3)$ | 7.52 | 7.22 | 54.5 | 45.3 | 59 | 41 | 3.5 | | |
| | $4^+(4)$ | 8.23 | | 15.4 | −9.2 | 18 | −6 | 0.3 | | |
| $^{34}$S | $0^+ \to 4^+(1)$ | 4.88 | 4.69 | 101.3 | 100.6 | 202 | 201 | 41 | | |
| | $4^+(2)$ | 6.90 | 6.25 | 58.4 | −44.4 | 65 | 37 | 4.2 | | |
| | $4^+(3)$ | 7.23 | | 37.6 | 59.1 | 86 | 107 | 7.4 | | |
| | $4^+(4)$ | 7.76 | | 56.8 | −34.6 | 68 | 23 | 4.6 | | |
| $^{38}$Ar | $0^+ \to 4^+(1)$ | 7.79 | 5.35 | −172.9 | 0 | −259 | −86 | 67 | | |
| | $4^+(2)$ | 14.88 | | −11.4 | 0 | −17 | −6 | 0.3 | | |

[a] From Ref. 21 except as noted.
[b] Reference 32.
[c] Reference 12.
[d] Reference 13.
[e] Reference 14.
[f] Reference 16.

TABLE VII. Selected $E4$ transitions in odd-even nuclei ($T = 1/2 \rightarrow T = 1/2$).

| | $J_i \rightarrow J_f$ | $E_f$ (MeV) th | $E_f$ (MeV) exp[a] | $A_p$ (fm$^4$) | $A_n$ (fm$^4$) | $M_p$ (fm$^4$) | $M_n$ (fm$^4$) | $B(E4)$ ($e^2$fm$^8 \times 10^3$) th | $B(E4)$ ($e^2$fm$^8 \times 10^3$) exp | Method of exp analysis |
|---|---|---|---|---|---|---|---|---|---|---|
| $^{19}$F | $\frac{1}{2}^+ \rightarrow \frac{7}{2}^+$ (1) | 4.64 | 4.38[b] | −13.1 | −2.3 | −21 | −10 | 0.44 | | |
| | $\frac{7}{2}^+$ (2) | 5.95 | 5.46[b] | −36.6 | −66.2 | −88 | −118 | 7.7 | | |
| | $\frac{7}{2}^+$ (3) | 6.43 | 6.07[b] | −26.6 | −35.1 | −57 | −66 | 3.2 | | |
| | $\frac{7}{2}^+$ (4) | 8.36 | | 10.7 | 23.2 | 28 | 40 | 0.8 | | |
| | $\frac{1}{2}^+ \rightarrow \frac{9}{2}^+$ (1) | 2.56 | 2.78[b] | 42.3 | 91.2 | 109 | 158 | 5.9 | 4.7±1.1[c] | PWBA |
| | $\frac{9}{2}^+$ (2) | 6.73 | 6.59[b] | −16.0 | −33.6 | 41 | 58 | 0.8 | | |
| | $\frac{9}{2}^+$ (3) | 8.27 | | 14.7 | −5.9 | 18 | −1.7 | 0.17 | | |
| | $\frac{9}{2}^+$ (4) | 10.74 | | −7.9 | 43.1 | 9.6 | 61 | 0.05 | | |
| $^{25}$Mg | $\frac{5}{2}^+ \rightarrow \frac{3}{2}^+$ (1) | 1.17 | 0.97 | −16.7 | −43.5 | −47 | −74 | 0.37 | | |
| | $\frac{3}{2}^+$ (2) | 3.08 | 2.80 | −16.9 | 19.2 | −16 | 20 | 0.043 | (1.5±0.4)[d,e] | PWBA |
| | $\frac{3}{2}^+$ (3) | 4.71 | 4.36 | −2.9 | −10.1 | −9 | −17 | 0.014 | | |
| | $\frac{3}{2}^+$ (4) | 6.04 | | 12.8 | 18.6 | 28 | 34 | 0.13 | | |
| | $\frac{5}{2}^+ \rightarrow \frac{5}{3}^+$ (2) | 2.06 | 1.96 | −27.3 | 16.4 | −33 | 11 | 0.18 | | |
| | $\frac{5}{2}^+$ (3) | 4.24 | 3.91 | 65.2 | 91.5 | 144 | 170 | 3.5 | 1.9±0.4[d] | PWBA |
| | $\frac{5}{2}^+$ (4) | 5.06 | | −6.6 | 0.6 | −10 | −2.4 | 0.017 | | |
| | $\frac{5}{2}^+ \rightarrow \frac{7}{2}^+$ (1) | 1.75 | 1.61 | −27.0 | −20.3 | −51 | −44 | 0.43 | | |
| | $\frac{7}{2}^+$ (2) | 3.02 | 2.74 | −59.1 | −101.8 | −140 | −182 | 3.3 | 1.5±0.4[d,e] | PWBA |
| | $\frac{7}{2}^+$ (3) | 5.18 | 5.01 | −42.7 | 12.1 | −58 | −3.2 | 0.56 | | |
| | $\frac{7}{2}^+$ (4) | 5.94 | 5.98 | −14.6 | −4.3 | −24 | −14 | 0.010 | | |
| | $\frac{5}{2}^+ \rightarrow \frac{9}{2}^+$ (1) | 3.62 | 3.41 | 13.0 | −5.4 | 17 | −1.7 | 0.05 | | |
| | $\frac{9}{2}^+$ (2) | 4.08 | 4.06 | 68.1 | 63.0 | 135 | 127 | 3.0 | 1.3±0.3[d] | PWBA |
| | $\frac{9}{2}^+$ (3) | 4.85 | 4.71 | −21.0 | 15.9 | −24 | 13 | 0.09 | | |
| | $\frac{9}{2}^+$ (4) | 6.56 | 5.97 | 54.1 | 66.1 | 115 | 125 | 2.2 | | |
| | $\frac{5}{2}^+ \rightarrow \frac{11}{2}^+$ (1) | 5.26 | (5.25) | 139.5 | 123.3 | 271 | 255 | 12.2 | 5.8±1.2[d] | PWBA |
| | | | | | | | | | 13±6[f] | DUELS[g] |
| | $\frac{11}{2}^+$ (2) | 5.80 | 5.53 | −6.1 | 6.2 | −6 | 6 | 0.006 | | |
| | $\frac{11}{2}^+$ (3) | 6.28 | (6.04) | 20.5 | −19.3 | 21 | −19 | 0.074 | | |
| | $\frac{11}{2}^+$ (4) | 7.70 | | 6.1 | −11.7 | 3.3 | −14 | 0.003 | | |
| | $\frac{5}{2}^+ \rightarrow \frac{13}{2}^+$ (1) | 5.73 | 5.46 | 37.0 | −0.2 | 56 | 17 | 0.5 | | |
| | $\frac{13}{2}^+$ (2) | 7.87 | | 17.1 | 19.1 | 34 | 37 | 0.2 | | |
| | $\frac{13}{2}^+$ (3) | 8.09 | | −85.0 | −54.6 | −154 | −125 | 3.9 | | |
| | $\frac{13}{2}^+$ (4) | 8.96 | | −38.9 | −26.7 | −71 | −76 | 0.8 | | |

[a] From Ref. 21 except where noted.
[b] Reference 32.
[c] Reference 18.
[d] Reference 19.
[e] The $\frac{3}{2}^+$ (2) and $\frac{7}{2}^+$ (2) states were not resolved in the electron scattering experiment of Ref. 19.
[f] Reference 15.
[g] Reference 16.

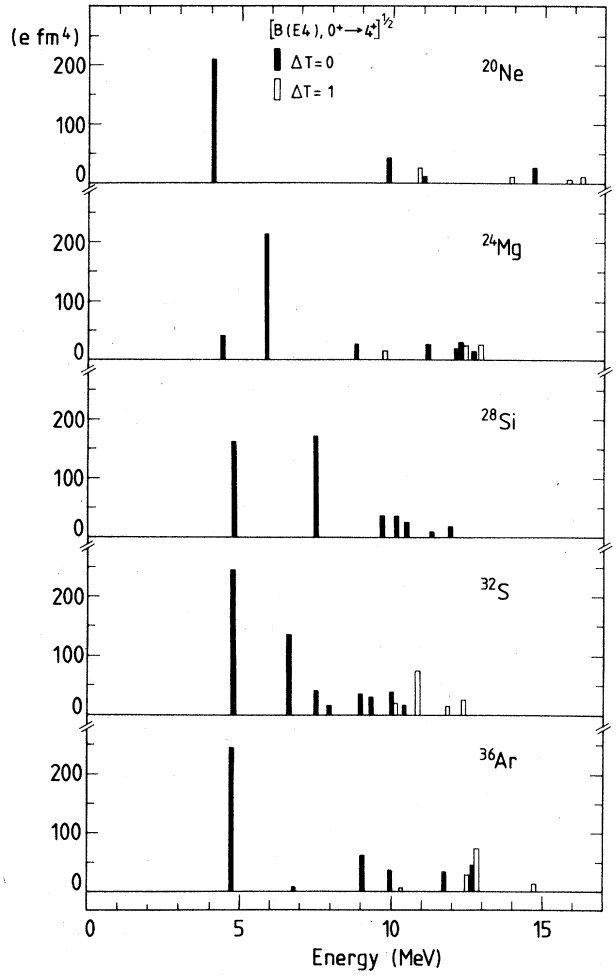


FIG. 1. Theoretical values for the $[B(E4), 0^+ \rightarrow 4^+]^{1/2}$ matrix elements as a function of excitation energy for $N=Z$ nuclei in the *sd* shell. Both $\Delta T=0$ and $\Delta T=1$ transitions are shown. The numbers are taken from Tables IV and V; $\Delta T=1$ transitions in $^{28}$S have not been calculated.

tions which have a very weak one-step $E4$ matrix element.

The calculated $E4$ strength distributions for $N=Z$ nuclei are shown in Fig. 1 and compared with experiment in Tables IV and V. The identities of the observed strong transitions in the $T=0$ nuclei $^{20}$Ne, $^{24}$Mg, and $^{28}$Si are correctly predicted, in particular the shift of the dominant $E4$ strength from the lowest $4^+$ state in $^{20}$Ne to the second $4^+$ state in $^{24}$Mg and back (partially) to the lowest $4^+$ state in $^{28}$Si. Moreover, the magnitudes of these three strong transitions are reproduced to within experimental error. To pursue this particular aspect of the $E4$ picture further it is important to obtain experimental measurements of the second $4^+$ state in $^{28}$Si, of the first two $4^+$ states in $^{32}$S, and of the first $4^+$ state in $^{36}$Ar. It would also be valuable to measure or to set experimental upper bounds on the strength of the higher excited $4^+$ states in the systems. Future experimental studies on these $T=0$ nuclei should also concentrate efforts on attempting the formidable task of extracting strengths for $\Delta T=1$ excitations to $J^\pi$, $T=4^+$, 1 states, the predictions for which are given in Table IV.

The predicted distributions of $E4$ strength in the $T_z=-1$ nuclei are more complex than for the $T_z=0$ systems and the individual values are smaller. The experimental data, single values for $^{18}$O and $^{22}$Ne and three values for $^{26}$Mg, confirm these predictions about fragmentation and average magnitudes, but except for $^{18}$O the experimental $B(E4)$ values tend to be larger than the predicted values by about 1 to 1.5 standard deviations. However, because of the varying structures of these excitations, this trend is not to be attributed to any simple isovector effective charge renormalization. More experimental measurements of $E4$ strength values of these systems would go far toward firmly validating the general picture of $E4$ strengths in $T=1$ systems predicted by the present stage of nuclear structure theory as well as to provide specific and unique information on the salient characteristics of the individual $J^\pi=4^+$ states.

The spectra of $E4$ excitations which can be obtained with odd-mass targets are, of course, potentially richer and more complex than for the $T_z=-1$, let alone the $T_z=0$ systems. Experimental electron scattering data have been reported for $^{19}$F (Ref. 18) and $^{25}$Mg (Refs. 15 and 19); results of our calculations for these two nuclei are presented in Table VII. Experiment and theory are in good agreement for the $\frac{1}{2}^+ \rightarrow \frac{9}{2}^+(1)$ transition in $^{19}$F; other $\frac{1}{2}^+ \rightarrow \frac{9}{2}^+ E4$ transitions up to 11 MeV in excitation are predicted to be weak. Only a few of the $\frac{5}{2}^+ \rightarrow J^\pi$ transitions in $^{25}$Mg are predicted to be strong and these are in general not to the lowest level of each spin. The relative strengths of the $B(E4)$ values reported by Okazaki *et al.* (Ref. 19) are in excellent agreement with the calculations. There is an overall factor of 2 discrepancy between experiment and theory. However, this is probably associated with the fact that a PWBA analysis was used by Okazaki *et al.* to extract the $E(E4)$ values (see the remarks in Sec. 5.5 of Ref. 15); the experimental $B(E4)$ which we have used for other nuclei have been obtained using a DWBA analysis.[16] Experimental results for two other transitions which are predicted to be strong in $^{25}$Mg have not been reported [the $\frac{5}{2}^+ \rightarrow \frac{9}{2}^+(2)$ and $\frac{5}{2}^+ \rightarrow \frac{13}{2}^+(3)$ transitions]. There is obviously an extensive amount of work to be done on this component of the $E4$ picture. Ultimately, the experimental delineation of the distributions

and magnitudes of $E4$ strength in odd-mass nuclei as a function of $A$, excitation energy, and final state spin, and the concurrent testing of the analogous nuclear structure model predictions will significantly enlarge our understanding both of nuclear wave functions and the foundations of the $E4$ excitation mode.

## IV. STRENGTH RATIOS FOR EXCITATION BY ELECTROMAGNETIC AND VARIOUS HADRONIC PROBES

In this section we derive some estimates of the matrix elements associated with inelastic hadron scattering and present some sample results for proton, alpha, and pionic probes. The calculations are based upon the assumption, which has proved to be remarkably successful in describing alpha scattering,[20] that the cross sections for hadronic excitation are proportional to the same matrix elements which enter into the calculations of electromagnetic transition rates. Thus these cross sections are proportional to

$$B'(a)=(2J_i+1)^{-1}[C_p(a)M_p+C_n(a)M_n]^2\,, \tag{16}$$

where $C_{p/n}$ represents the interaction strengths of probe $(a)$ with the protons/neutrons of the nucleus.

Since we are concerned here with nuclear structure effects rather than the details of the probe-specific absolute interaction strengths we choose to work with normalized strength factors $B(a)$ defined so as to yield a value for $T=0\rightarrow T=0$ transitions (for which $M_p-M_n=0$) which is unique, independent of probe $(a)$:

$$B(a)=B'(a)/[C_p(a)+C_n(a)]^2$$
$$=(2J_i+1)^{-1}[\tfrac{1}{2}(M_p+M_n)+\tfrac{1}{2}R(a)(M_p-M_n)]^2\,, \tag{17}$$

where

$$R(a)=\frac{C_p(a)-C_n(a)}{C_p(a)+C_n(a)}\,. \tag{18}$$

For the electromagnetic probes, $C_p=e$ and $C_n=0$ and hence $R(a=e)=1$, and Eq. (17) reduces to Eq. (6),

$$B(E4)=B(e)=(2J_i+1)^{-1}M_p{}^2\,. \tag{19}$$

For the alpha particle, $C_p=C_n$ and hence $R(a=\text{alpha})=0$ and

$$B(\text{alpha})=(2J_i+1)^{-1}[\tfrac{1}{2}(M_p+M_n)]^2\,. \tag{20}$$

For pions at energies near the (3,3) resonance $R(a=\pi^{\pm})=\pm 0.5$ and

$$B(\pi^{\pm})=(2J_i+1)^{-1}[\tfrac{1}{2}(M_p+M_n)\pm\tfrac{1}{4}(M_p-M_n)]^2\,. \tag{21}$$

Pion inelastic scattering experiments are currently designed to yield the ratios of excitation strengths with $\pi^-$ and $\pi^+$ projectiles. This quantity is expressed in our model as

$$\frac{B(\pi^-)}{B(\pi^+)}=\left(\frac{M_p+3M_n}{3M_p+M_n}\right)^2\,. \tag{22}$$

This precise result depends, of course, upon the assumption that near resonance the $\pi^-$-$n$ and $\pi^+$-$p$ interaction amplitudes are 3.0 times stronger than the $\pi^-$-$p$ and $\pi^+$-$n$ amplitudes, but analogous expressions are easily obtained for different assumptions about these elementary-particle features.

Many strongly excited $4^+$ states at high excitation energy have been reported in alpha inelastic scattering experiments. In Table VIII are listed some strengths from alpha scattering on $^{24}$Mg (Ref. 20) in comparison with the present theoretical predictions for the first nine $4^+$ states. Above 9.0 MeV there is complete disagreement between experiment and theory. This could be due to experimental errors in the spin assignments (in Endt and van der Leun[21] no definite $4^+$ assignments have been made above 9.0 MeV) or to two-step contributions to the inelastic scattering cross sections which were not considered in the DWBA analysis, rather than a failure of the nuclear structure wave functions.

Some predicted values for $B(\alpha)$ and $B(\pi^{\pm})$ in $T_z=-1$ nuclei are given in Table IX. It should be quite interesting to carry out the corresponding experimental measurements since several quite strong deviations from isoscalar behavior are predicted. Inelastic alpha scattering to $4^+$ states in $^{22}$Ne and $^{26}$Mg as well as in several $N=Z$ nuclei has been measured by Rebel *et al.*[22] but the extraction of $B(\alpha)$ values via the methods of Ref. 20 have not been carried out.

As a final example of hadronic excitations we compare some experimentally measured proton

TABLE VIII. Alpha scattering transition strengths for $0^+\rightarrow 4^+$ transitions in $^{24}$Mg.

| $J_f(T_f)$ | Energy (MeV) th | Energy (MeV) exp[a] | $B$(alpha) (fm$^8\times 10^3$) th | $B$(alpha) (fm$^8\times 10^3$) exp[a] |
|---|---|---|---|---|
| $4^+(0)$ | 4.42 | 4.12 | 1.6 | |
| $4^+(0)$ | 5.89 | 6.01 | 44.0 | $21.4\pm 3.2$ |
| $4^+(0)$ | 8.79 | 8.64 | 0.6 | $3.0\pm 0.5$ |
| $4^+$ | | 9.12 | | $8.1\pm 1.4$ |
| $(4^+)$ | | 9.30 | | $12.2\pm 1.9$ |
| $4^+$ | | 10.03 | | $16.0\pm 2.4$ |
| $4^+(0)$ | 9.62 | | 0.002 | |
| $4^+(1)$ | 9.74 | | | |
| $4^+(0)$ | 11.15 | | 0.6 | |
| $4^+(0)$ | 12.17 | | 0.3 | |
| $4^+(0)$ | 12.24 | | 0.7 | |
| $4^+(1)$ | 12.28 | | | |

[a] $B(\text{alpha})=(A/2Z)^2B(IS)$ where $B(IS)$ are taken from Table IX in Ref. 20.

TABLE IX. Alpha scattering and pion scattering strengths for the $0^+ \rightarrow 4^+$ transitions in $T_z = -1$ nuclei.

| Nucleus | $J_i \rightarrow J_f$ | $B$(alpha) (fm$^8 \times 10^3$) | $\frac{B(\text{alpha})}{B(E4)}$ | $\frac{B(\pi^-)}{B(\pi^+)}$ |
|---|---|---|---|---|
| $^{18}$O | $0^+ \rightarrow 4^+(1)$ | 11.5 | 4.00 | 2.78 |
| $^{22}$Ne | $0^+ \rightarrow 4^+(1)$ | 4.7 | 0.38 | 0.28 |
| | $4^+(2)$ | 11.7 | 1.37 | 1.34 |
| $^{26}$Mg | $0^+ \rightarrow 4^+(1)$ | 13.7 | 0.80 | 0.80 |
| | $4^+(2)$ | 16.9 | 1.20 | 1.19 |
| $^{30}$Si | $0^+ \rightarrow 4^+(1)$ | 20.7 | 1.77 | 1.65 |
| | $4^+(2)$ | 31.8 | 0.78 | 0.77 |
| $^{34}$S | $0^+ \rightarrow 4^+(1)$ | 40.8 | 1.00 | 1.00 |
| | $4^+(2)$ | 0.2 | 0.05 | 0.09 |
| $^{38}$Ar | $0^+ \rightarrow 4^+(1)$ | 30.0 | 0.44 | 0.36 |

scattering strengths in $^{26}$Mg (Ref. 23) with estimates for 30 MeV proton scattering. From the microscopic optical model of Brieva and Rook[24] we obtain values for the interaction strengths at this energy of $C_p = 0.3$ and $C_n = 0.7$. This yields

$$B(\text{proton}, 30\ \text{MeV}) = (2J_i + 1)^{-1}(0.3M_p + 0.7M_n)^2. \quad (23)$$

The predicted and measured $B$ values are presented in Table X. The experimental $0^+ \rightarrow 4_2^+$ strength is twice as large as the predicted value. This is probably a real discrepancy since, in addition, the experimental electron scattering $B(E4)$ value is larger than predicted (see Table V). The predicted ratio $B(p)/B(E4)$ is consistent with experiment. The situation for the weaker $0^+ \rightarrow 4_1^+$ transition is not so clear since the $B(E4)$ value has not yet been extracted from the experimental data; the calculated $B(p)$ value is in fair agreement with experiment. The proton scattering strength to the third $4^+$ state is predicted to be much stronger than the electromagnetic excitation strength.

## V. SUMMARY AND CONCLUSIONS

The Chung-Wildenthal wave functions for the $sd$-shell nuclei have been used to calculate hexadecapole transition densities. These have been combined with harmonic-oscillator radial wave functions to predict proton and neutron $E4$ matrix elements within the $sd$-shell model space. There is at present no good theoretical prescription for obtaining radial wave functions for open-shell nuclei which are more realistic than those of the harmonic-oscillator potential.

The effects of model-space truncation on the $E4$ operator have been taken into account by introducing empirical effective charges. The experimental values for strong electromagnetic excitations are all consistent with a isoscalar effective charge of $e_p + e_n \simeq 2.0e$. This is much larger than the results of microscopic core-polarization calculations of Horikawa *et al.*,[7] which gave $e_p + e_n \simeq 1.15e$.

These empirical effective charges were used to calculate the proton and neutron matrix elements $M_p$ and $M_n$; electromagnetic excitation strengths are determined by $M_p$ while hadronic scattering strengths depend on both $M_p$ and $M_n$. Predicted electromagnetic $B(E4)$ values are in good agreement with existing experiments over a wide range of magnitudes. However, experimental electron scattering results are lacking for the upper $sd$ shell as well as for pure $\Delta T = 1$ excitations in $N = Z$ nuclei.

It is more difficult to extract nuclear structure information from the hadronic scattering cross sections. For transitions which are characterized by small direct matrix elements, two-step contributions are certainly important; this may be responsible for the disagreement between the very small isoscalar excitation strengths predicted to $4^+$ states above 9 MeV in $^{24}$Mg compared with experiment. A systematic analysis of alpha, proton, or pion scattering for $0^+ \rightarrow 4^+$ transitions in many $sd$-shell nuclei is needed to confirm our predic-

TABLE X. Proton scattering transition strengths $B(p) = B$(proton, 30 MeV) for the $0^+ \rightarrow 4^+$ transitions in $^{26}$Mg.

| Energy (MeV) th | Energy (MeV) exp[a] | $B(p)$ (fm$^8 \times 10^3$) th[b] | $B(p)$ (fm$^8 \times 10^3$) exp[c] | $B(p)/B(E4)$ th | $B(p)/B(E4)$ exp[d] |
|---|---|---|---|---|---|
| 4.59 | 4.32 | 12.5 | 18±2 | 0.74 | |
| 5.41 | 4.90 | 18.1 | 41±2 | 1.28 | 1.6±0.3 |
| 5.87 | 5.47 | 6.5 | | 5.0 | |
| 6.13 | 5.72 | 3.3 | | 0.38 | |

[a] Reference 21.
[b] $B(p) = (0.3M_p + 0.7M_n)^2$.
[c] Reference 23.
[d] For $B(E4)_{\text{exp}}$ see Table VI.

TABLE XI. Hartree-Fock results for $^{20}$Ne.

| | Harmonic oscillator | Hartree-Fock Skyrme III | Hartree-Fock Skyrme IV |
|---|---|---|---|
| $\langle d_{5/2}\|r^4\|d_{5/2}\rangle_p$ (fm$^4$)[a] | 179 | 181 | 198 |
| $\langle d_{5/2}\|r^4\|d_{3/2}\rangle_p$ (fm$^4$)[a] | 179 | 236 | 274 |
| $r_p$ (fm)[b] | 2.905 | 2.905 | 2.902 |
| $BE(d_{5/2})_p$ (MeV)[c] | | −5.42 | −5.62 |
| $BE(d_{3/2})_p$ (MeV)[c] | | −0.02 | 0.78 |

[a] Proton radial-matrix elements.
[b] Point proton rms radii.
[c] Proton single-particle energies.

tions for the relative sizes and phases of the proton and neutron matrix elements.

## APPENDIX

In this section we discuss the Hartree-Fock calculations for $^{20}$Ne and $^{36}$Ar which have recently been carried out by Brown and Massen.[6] For these calculations a Skyrme interaction[25] was used and a self-consistent spherical potential was constructed out of the monopole densities obtained by adding the squares of the radial wave functions weighted by the orbit occupation probabilities, which in turn had been obtained from the $sd$-shell-model calculations. The spin-orbit parameter was chosen to reproduce the $d_{5/2}$-$d_{3/2}$ spin-orbit splitting of about 5 MeV in $A = 17$.

The results using Skyrme III and Skyrme IV interactions for $^{20}$Ne are given in Table XI. Under the column labeled "harmonic oscillator" we give the $r^4$ matrix elements which we would obtain if we took the theoretical value of $r_p = 2.905$ fm and interpreted it as a sum of harmonic oscillators to extract $b$ and then to calculate $\langle r^4\rangle = 15.75b^4$. For the $d_{5/2}$ orbit the Hartree-Fock results are very close to the harmonic-oscillator results, but the Hartree-Fock results for the off-diagonal, $d_{5/2}$-$d_{3/2}$ matrix element are much larger than the harmonic-oscillator result and they depend strongly on the value of the binding energy. (The radial wave function for the unbound $d_{3/2}$ state obtained with the Skyrme IV interaction was obtained by the method described by Beiner *et al.*[25])

The experimental separation energies of the $d_{5/2}$ and $d_{3/2}$ orbits in $^{20}$Ne, −16.87 and −18.42 MeV, respectively, are very different from the Hartree-Fock single-particle energies because of the residual interactions. Thus, the tails of the wave functions, which are important for the $r^4$ matrix elements and which are determined by the separation energy, cannot be reliably calculated with spherical Hartree-Fock or any other smoothly mass dependent single-particle wave functions. These large separation energies may even result in $\langle r^4\rangle$ matrix elements which are smaller than the harmonic-oscillator results. There is at present no rigorous theoretical prescription for taking the residual interactions into account.

The situation is different when the orbits are more deeply bound. In Table XII the Hartree-Fock

TABLE XII. Hartree-Fock results for $^{36}$Ar.[a]

| | Harmonic oscillator | Hartree-Fock Skyrme III | Hartree-Fock Skyrme IV |
|---|---|---|---|
| $\langle d_{5/2}\|r^4\|d_{5/2}\rangle_p$ (fm$^4$) | 220 | 201 | 196 |
| $\langle d_{5/2}\|r^4\|d_{3/2}\rangle_p$ (fm$^4$) | 220 | 213 | 219 |
| $r_p$ (fm) | 3.318 | 3.318 | 3.298 |
| $BE(d_{5/2})_p$ (MeV) | | −13.51 | −17.52 |
| $BE(d_{3/2})_p$ (MeV) | | −7.26 | −6.93 |

[a] See footnotes to Table XI.

results for $^{36}$Ar are given. For both Skyrme III and Skyrme IV the results are close to the harmonic-oscillator values, even though the $d_{5/2}$ single-particle energies are quite different in the two cases. In this case the experimental separation energies for the $d_{5/2}$ and $d_{3/2}$ orbits of −17.01 and −15.25 MeV, respectively, are fairly close to the Hartree-Fock single-particle energies.

ACKNOWLEDGMENTS

This material is based upon work supported in part by the U. S. National Science Foundation under Grant No. Phy-7822696. One of the authors (B.H.W.) wishes to thank Prof. K. W. Allen and Dr. P. E. Hodgson for their hospitality during his stay at Oxford.

*Permanent address.

[1]W. Chung, thesis, Michigan State University, 1976 (unpublished); W. Chung and B. H. Wildenthal (unpublished).

[2]B. H. Wildenthal, *Elementary Modes of Excitation in Nuclei*, edited by R. Broglia and A. Bohr (Soc. Italiana de Fisica, 1977); B. H. Wildenthal and W. Chung, *Mesons in Nuclei*, edited by M. Rho and D. H. Wilkinson (North-Holland, Amsterdam, 1979); B. A. Brown, W. Chung, and B. H. Wildenthal, Phys. Rev. Lett. 40, 1631 (1978); B. H. Wildenthal, Nucleonika 23, 459 (1978).

[3]J. L. Friar and J. W. Negele, *Advances in Nuclear Physics*, edited by M. Baranger and E. Vogt (Plenum, New York, 1975), Vol. 8, p. 219.

[4]L. J. Tassie and F. C. Barker, Phys. Rev. 111, 940 (1958).

[5]R. J. Philpott, W. T. Pinkston, and G. R. Satchler, Nucl. Phys. A119, 241 (1968); G. M. McAllen, W. T. Pinkston, and G. R. Satchler, Part. Nucl. 1, 412 (1971); A. Prakash and N. Austern, Ann. Phys. (N.Y.) 51, 418 (1969).

[6]B. A. Brown and S. E. Massen (unpublished).

[7]Y. Horikawa, T. Hoshino, and A. Arima, Phys. Lett. 63B, 134 (1976).

[8]D. F. Geesaman, R. L. McGrath, J. W. Noé, and R. E. Malmin, Phys. Rev. C 19, 1938 (1979); H. Sagawa, *ibid.* 19, 506 (1979).

[9]L. J. Tassie, Aust. J. Phys. 9, 407 (1956); 11, 481 (1958).

[10]R. P. Singhal, H. S. Caplan, J. R. Moreira, and T. E. Drake, Can. J. Phys. 51, 2125 (1973).

[11]H. Zarek, S. Yen, B. O. Pich, T. E. Drake, C. F. Williamson, S. Kowalski, C. P. Sargent, W. Chung, B. H. Wildenthal, M. Harvey, and H. C. Lee, Phys. Lett. 80B, 26 (1978).

[12]B. E. Norum, thesis, Massachusetts Institute of Technology, 1979 (unpublished).

[13]X. K. Maruyama, F. J. Kline, J. W. Lightbody, S. Penner, W. J. Briscoe, M. Lunnan, and H. Crannell, Phys. Rev. C 19, 1624 (1979).

[14]E. W. Lees, A. Johnson, S. W. Brain, C. S. Curran, W. A. Gillespie, and R. P. Singhal, J. Phys. A 7, 936 (1974).

[15]E. W. Lees, C. S. Curran, T. E. Drake, W. A. Gillespie, A. Johnston, and R. P. Singhal, J. Phys. G 5, 341 (1976).

[16]S. T. Tuan, L. E. Wright, and D. S. Onley, Nucl. Instrum. Methods 60, 70 (1968).

[17]A. Nakada and Y. Torizuka, J. Phys. Soc. Jpn. 32, 1 (1972).

[18]M. Oyamada, T. Terasawa, K. Nakahara, Y. Endo, H. Saito, and E. Tanaka, Phys. Rev. C 11, 1578 (1975).

[19]Y. Okazaki, K. Hayakawa, K. Nakahara, M. Oyamada, T. Terasawa, and H. Saito, Phys. Lett. 55B, 373 (1975).

[20]A. M. Bernstein, *Advances in Nuclear Physics*, edited by M. Baranger and E. Vogt (Plenum, New York, 1969), Vol. 3, p. 325.

[21]P. M. Endt and C. van der Leun, Nucl. Phys. A235, 27 (1974).

[22]H. Rebel, G. W. Schweimer, G. Schatz, J. Specht, R. Löhken, G. Hauser, D. Habs, and H. Klewe-Nebenius, Nucl. Phys. A182, 145 (1972).

[23]P. W. F. Alons, H. P. Blok, and J. F. A. van Hienen, Phys. Lett. 83B, 34 (1979).

[24]F. A. Brieva and J. R. Rook, Nucl. Phys. A307, 493 (1978).

[25]M. Beiner, H. Flocard, N. van Giai, and P. Quentin, Nucl. Phys. A238, 29 (1975).

[26]M. Miska, B. Norum, M. W. Hynes, W. Bertozzi, S. Kowalski, F. N. Rad, C. P. Sargent, T. Sasanuma, and B. L. Berman, Phys. Lett. 83B, 165 (1979).

[27]L. A. Schaller, T. Dubler, K. Kaeser, G. A. Rinker, B. Robert-Tissot, L. Schellenberg, and H. Schneuwly, Nucl. Phys. A300, 225 (1978).

[28]C. W. de Jager, H. de Vries, and C. de Vries, At. Data Nucl. Data Tables 14, 479 (1974).

[29]C. G. Li, M. R. Yearian, and I. Sick, Phys. Rev. C 9, 1861 (1974); I. Sick, private communication.

[30]H. Euteneuer, H. Rothhaas, O. Schwentker, J. R. Moreira, C. W. de Jager, L. Lapikas, H. de Vries, J. Flanz, K. Itoh, G. A. Peterson, D. V. Webb, W. C. Barber, and S. Kowalski, Phys. Rev. C 16, 1703 (1977).

[31]R. Engfer, H. Schneuwly, J. L. Vuilleumier, H. K. Walter, and A. Zehnder, At. Data Nucl. Data Tables 14, 509 (1974).

[32]F. Ajzenberg-Selove, Nucl. Phys. A300, 1 (1978).